Integrated multimodal microfluidic E-skin powered by synergistic tandem nanogenerators for sweat health monitor and skin temperature analysis

Kai HAN[1], Dadong ZHANG[1], Wenbo ZHUANG, Yanfen WAN, Peng YANG**

National Center for International Research on Photoelectric and Energy Materials, Yunnan Key Laboratory for Micro/Nano Materials & Technology, School of Materials and Energy, Yunnan University, Kunming 650091, China. E-mail: yfwan@ynu.edu.cn, pyang@ynu.edu.cn.

Schematic 1: The principle of hydrovoltaic-electric generation (HEG) is that when an aqueous solution makes contact with a solid with surface charge, the interfacial interaction is dominated by an electric double layer (EDL). This EDL is composed of a surface ion layer firmly adsorbed on the solid, known as the Stern layer, as well as a layer rich in counterions attracted to the surface charge, known as the diffusion layer. The EDL creates a strong electric field, resulting in a sharp potential gradient across it[1]. The principle of moist-electric generation (MEG) is that in the electricity generation process, materials bearing hydrophilic functional groups (e.g., –OH, –COOH, and –SO3H) initially absorb water molecules. Second, the aggregation of water molecules in materials leads to the dissociation of functional groups, which weakens and breaks the polar chemical bonds, releasing numerous positively and/or negatively charged ions, and accordingly resulting in a concentration difference in the specific region. Third, electric potential occurs as a result of separated positively and negatively charged ions. The positively or negatively charged functional groups can be immobilized because of their large volume or by bonding with skeletons in materials, while the counter charged ions can freely move as carriers. The mobile carriers transport from the high concentration region to the low concentration region, thus inducing charge separation in functional materials and producing voltage or an electric current. Finally, the chemical potential energy (ΔE) from water molecule absorption on materials is converted into electric potential power. Unlike HEG, MEG can produce electricity from ubiquitous air, avoiding the physical contact between water and materials that could induce the damage of materials as well as the geographic limitations for practical applications.

Table S1. Raman Data of PPC after sulfuric acid and chloroacetic acid treatment.

Name	I_D	I_G	I_D/I_G
PPC treated by chloroacetic acid	747.44	763.44	0.98
PPC treated by sulfuric acid	636.83	663.33	0.96

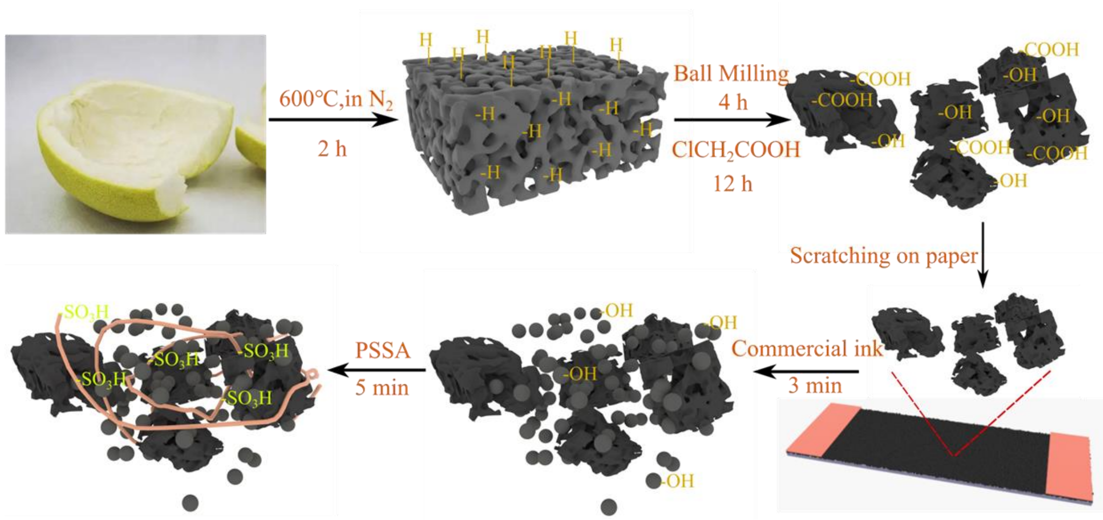

Figure S1. The preparation process of PPC materials. The pomelo peel is firstly made into toner, then ball milled and further treated with chloroacetic acid. Then, the treated toner is used to coat a piece of paper then soaked in ink and PSSA to obtain the final device.

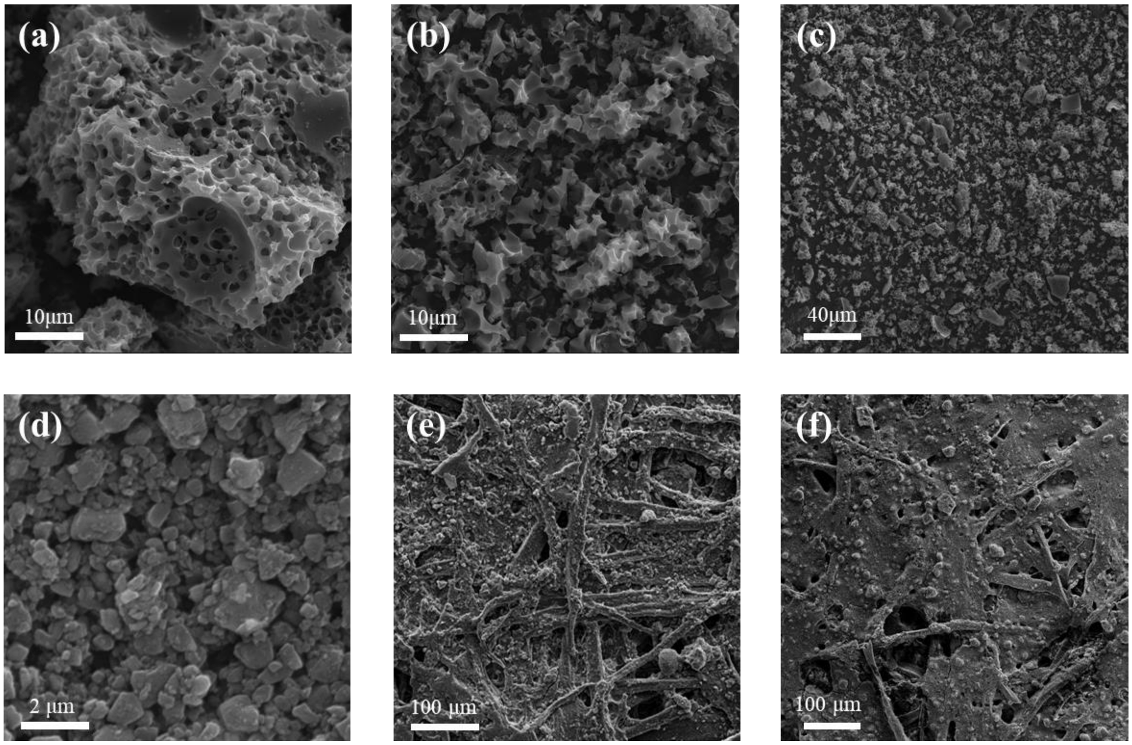

Figure S2. SEM photos of PPC particles: (a) particle without ball milling, (b)(c)particle after ball milling. SEM photo of PPC paper device: (d) PPC surface without soaking ink, (e) PPC surface soaked with ink, (f) PPC surface soaked with ink and PSSA.

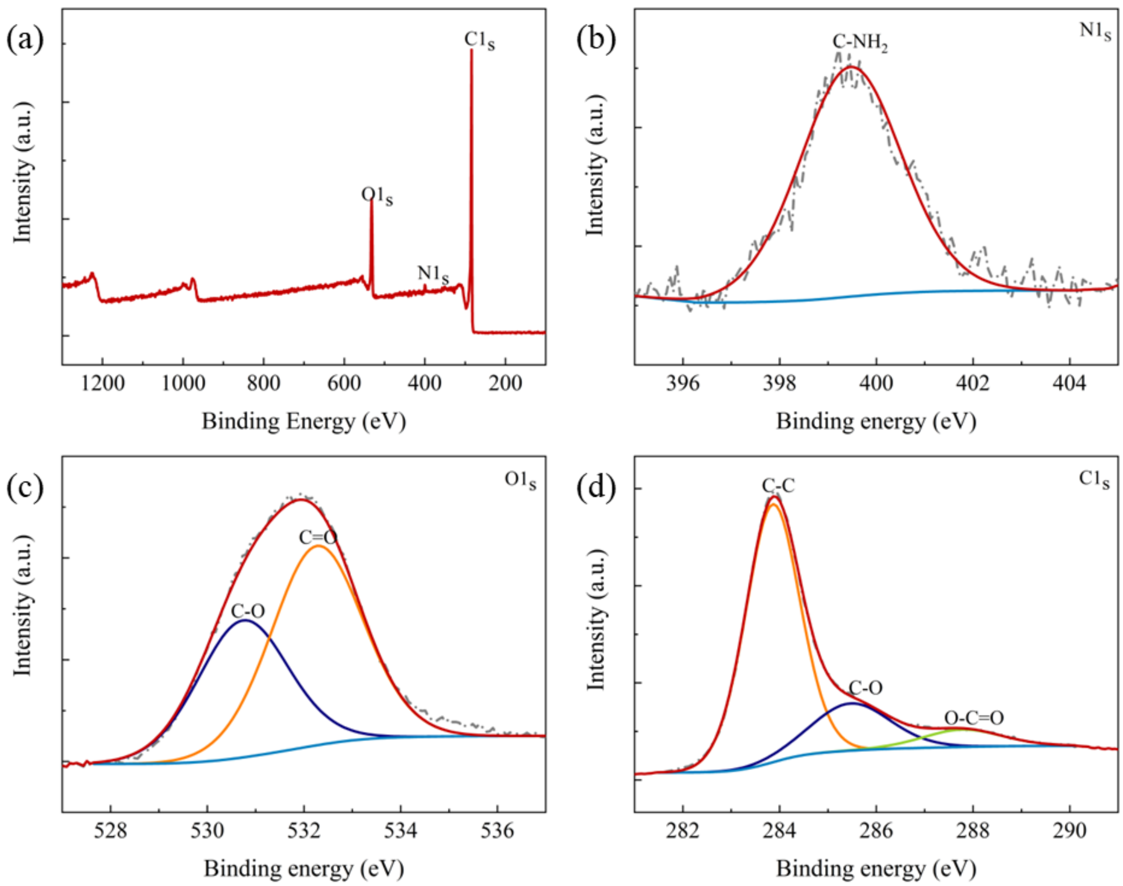

Figure S3. (a)(b)(c)(d) XPS spectrum of pomelo peel carbon material treated with chloroacetic acid, and the groups corresponding to the peak positions are shown in the figure. The results show that the surface contains not only hydroxyl groups, but also carboxyl groups.

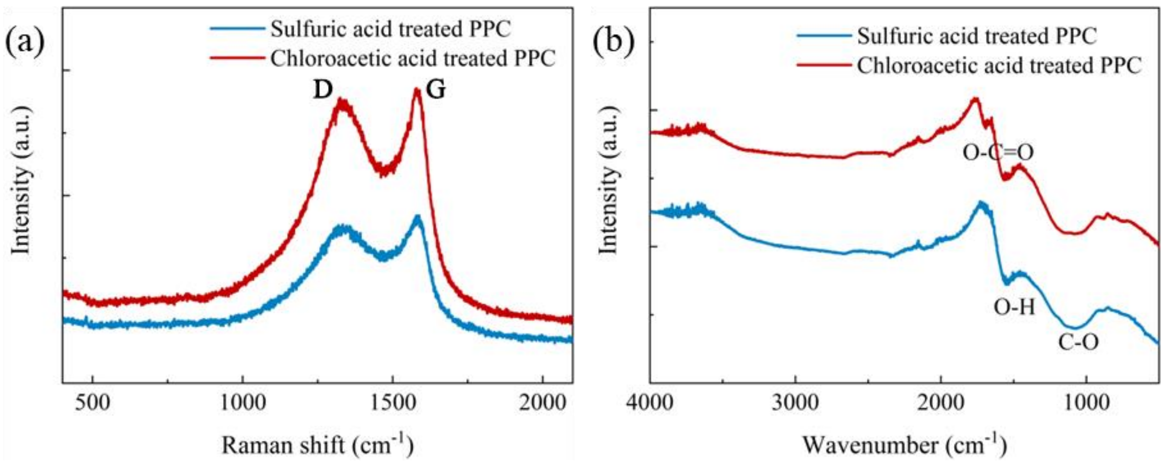

Figure S4. (a) Raman spectra of grapefruit peel carbon treated with different acids; (b) Fourier transform infrared spectra of grapefruit peel carbon treated with different acids.

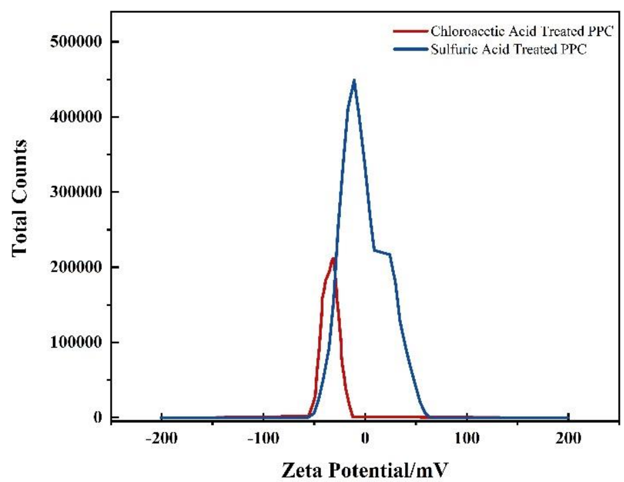

Figure S5. Zeta potential of pomelo peel carbon treated with chloroacetic acid and sulfuric acid.

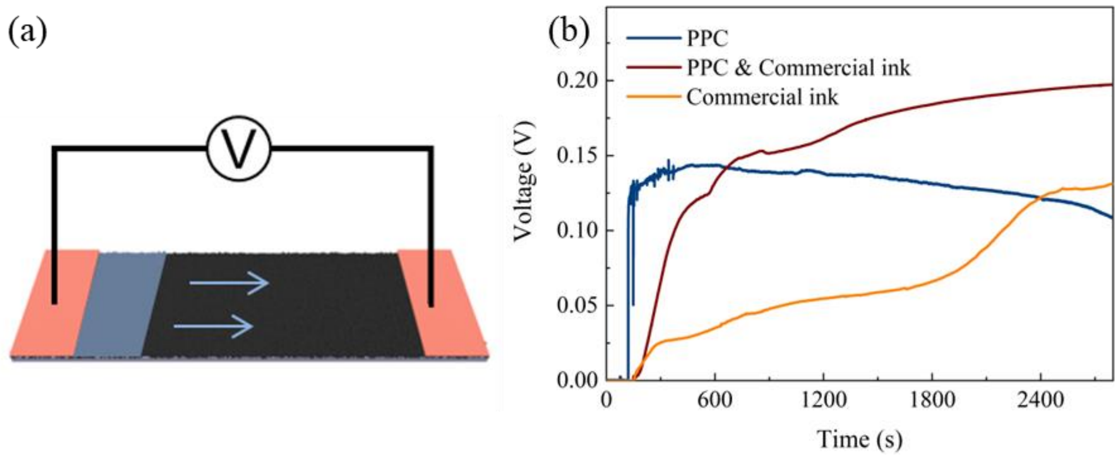

Figure S6. (a)Schematic diagram of the test of PPC hydrovoltaic-electric generation device; (b)the influence of different materials on the hydrovoltaic-electric generation performance of the device.

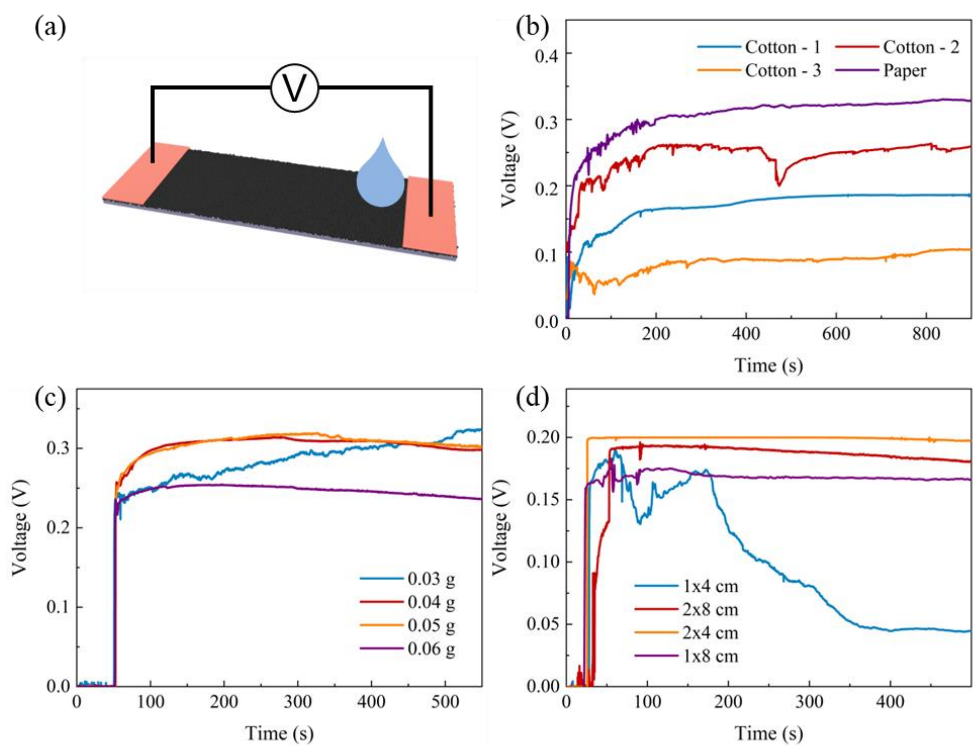

Figure S7. (a)Schematic diagram of the device; (b-d)Effects of substrate, carbon particle loading and size on the hydrovoltaic performance of the device.

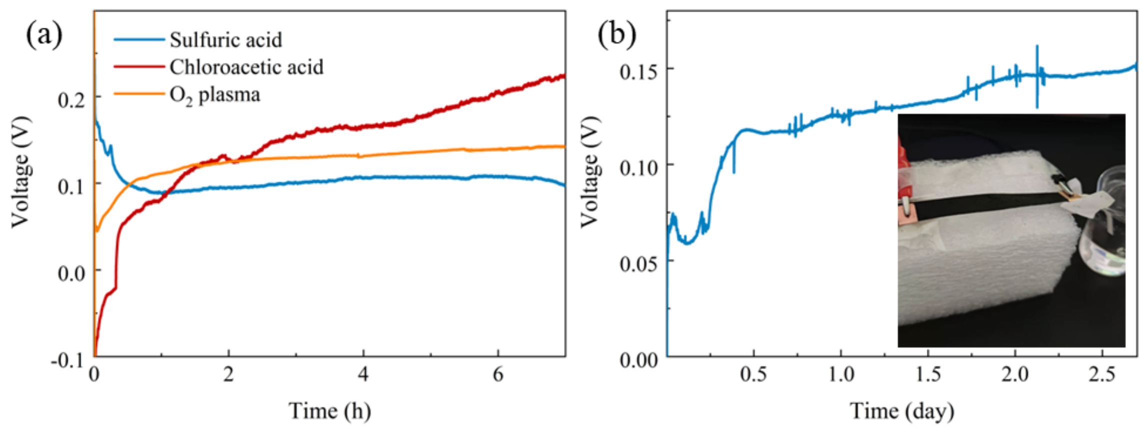

Figure S8. Hydrovoltaic test of continuous water supply (a)Continuous water supply voltage output of different surface modification devices; (b)In the case of continuous water supply, open circuit voltage output of chloroacetic acid treated devices (inset: photo of test device).

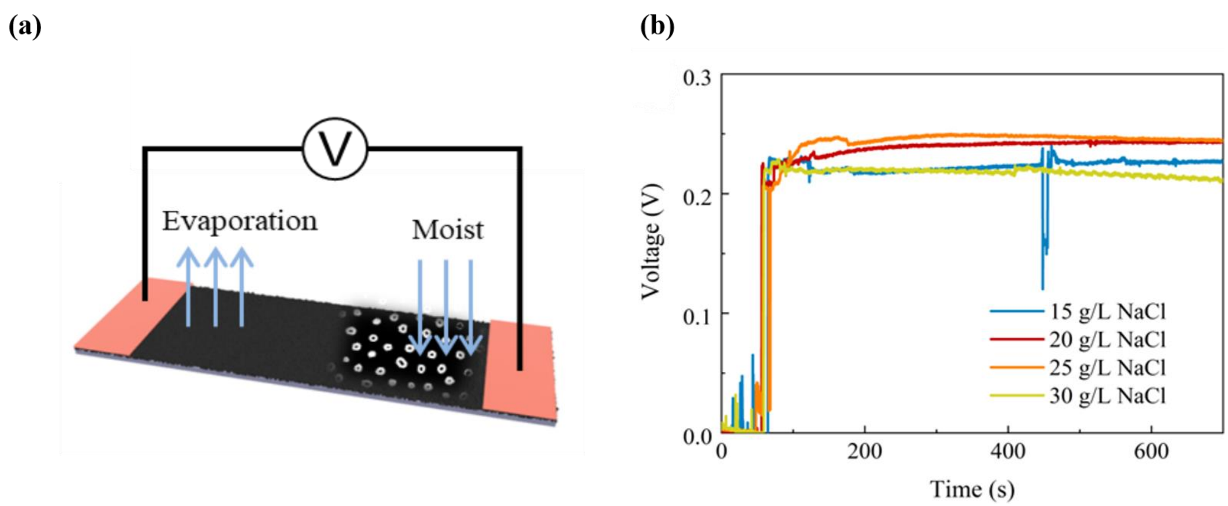

Figure S9. (a)Schematic diagram of the device. (b) The output voltage responses to PPC hydrovoltaic device to simulated sweat with different NaCl concentrations.

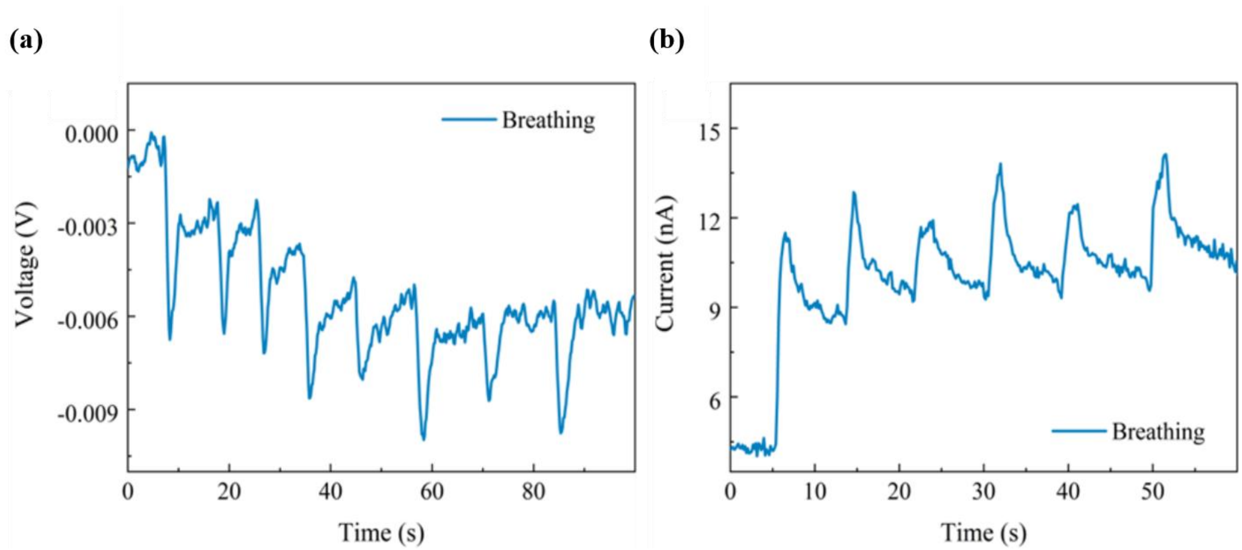

Figure S10. The open (a) circuit voltage and (b) short-circuit current of the device during breathing after dripping with simulated seawater.

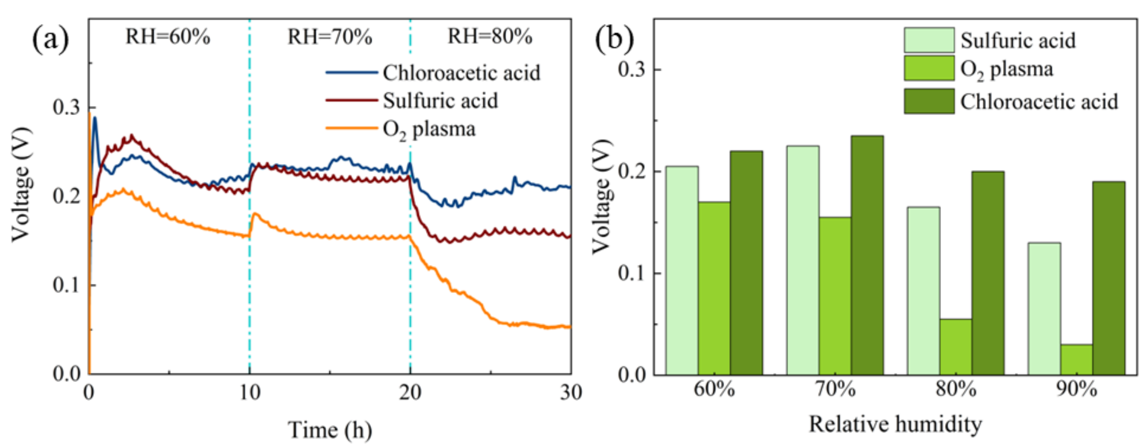

Figure S11. (a)The effect of different surface modification treatments on the moist-electric generation performance of the device; (b)The output open circuit voltage of the device under different humidity conditions for moist-electric generation.

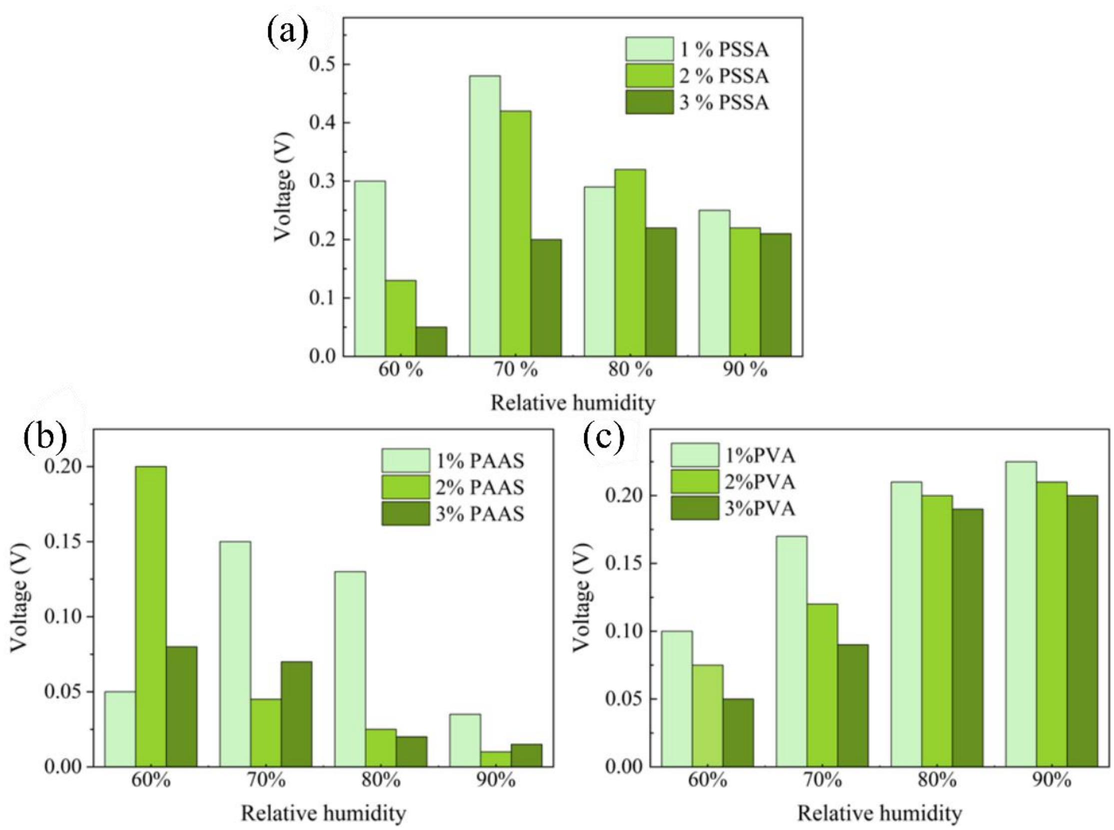

Figure S12. The open circuit voltages output of PPC devices treated with PSSA、PAAS and PVA at the different humidity.

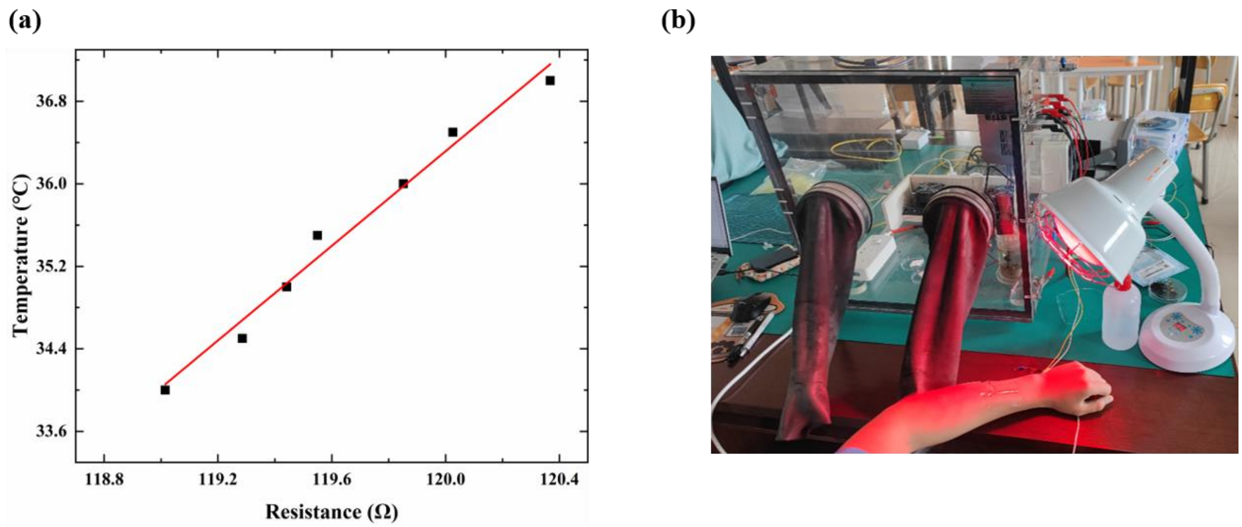

Figure S13. (a) The surface temperature of human skin measured through the resistance of the thermistor powered by the moist-electric generator integrated in the SE-skin. (b) The measurement of the surface temperature of human skin.

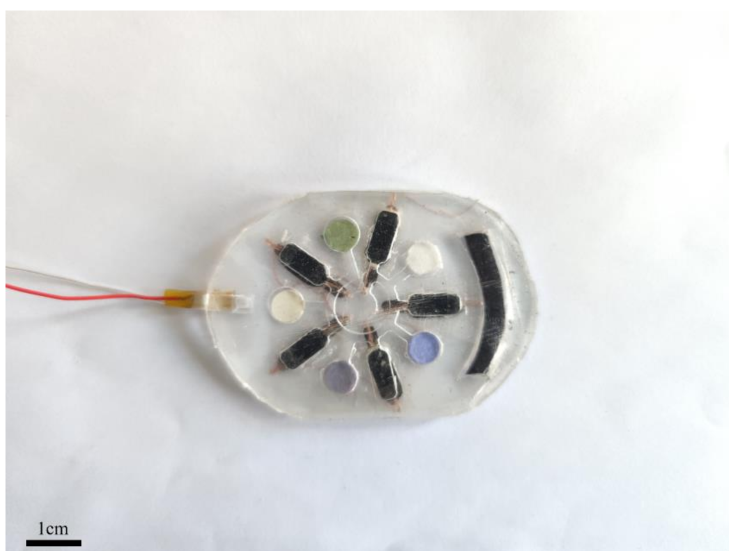

Figure S14. The physical picture of flexible electronic device.

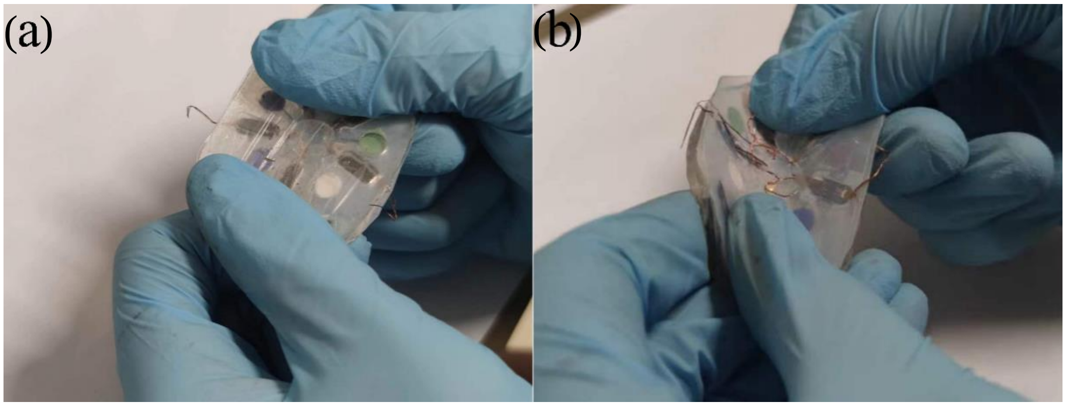

Figure S15. The flexible electronic device (a) stretch and (b) twist.